Mathematical and Computational Applications

MDPI

Article

Stability Analysis via a Neurodynamic Approach with Time-Varying Coefficients for Solving Inverse Quasi-Variational Inequality Problems

Vajahat Karim Khan [1], Md. Kalimuddin Ahmad [1] and Adnène Arbi [2,*]

[1] Department of Mathematics, Aligarh Muslim University, Aligarh 202002, Uttar Pradesh, India; gh7904@myamu.ac.in (V.K.K.); ahmad_kalimuddin@yahoo.co.in (M.K.A.)
[2] Laboratory of Engineering Mathematics (LR01ES13), Tunisia Polytechnic School, University of Carthage, B.P. 743, La Marsa 2078, Tunisia
* Correspondence: adnen.arbi@enseignant.edunet.tn

Abstract

This paper proposes finite-time (FT) and fixed-time (FXT) neurodynamic models with time-varying coefficients for solving inverse quasi-variational inequality problems (IQVIPs). Two projected models with time-dependent gains are developed to enhance convergence speed and transient performance. A nominal model establishes the equivalence between equilibrium points and IQVIP solutions. Under Lipschitz continuity and strong monotonicity assumptions, the existence, uniqueness, and global convergence of the proposed models are ensured. By employing Lyapunov stability theory, finite-time and fixed-time convergence of the continuous-time models are rigorously established, where explicit settling-time bounds independent of initial conditions are derived for the FXT case. Furthermore, the robustness of the proposed models under bounded disturbances is analyzed. To validate the theoretical findings, a discrete-time implementation based on the forward Euler method is developed. Numerical experiments demonstrate that all trajectories converge within a uniform upper bound, showing convergence behavior consistent with the fixed-time characteristics of the continuous-time model. Although the convergence time varies with initial conditions, it remains uniformly bounded, which is consistent with the fixed-time stability characteristics of the continuous-time model. The proposed framework provides a computationally efficient and scalable approach for solving IQVIPs, with potential applications in traffic equilibrium, communication networks, distributed control systems, and multi-agent coordination. Its adaptive structure and fixed-time convergence properties make it particularly suitable for real-time optimization in dynamic and uncertain environments.

Keywords: finite-time stability; fixed-time stability; neurodynamic approach; time-varying coefficients; inverse quasi-variational inequality problem; real-time optimization

Check for updates

Academic Editor: Gianluigi Rozza

Received: 1 May 2026
Revised: 20 May 2026
Accepted: 27 May 2026
Published: 1 June 2026

Copyright: © 2026 by the authors. Licensee MDPI, Basel, Switzerland. This article is an open access article distributed under the terms and conditions of the Creative Commons Attribution (CC BY) license.

1. Introduction

Suppose $\mathbb{R}^k$ denotes k-dimensional Euclidean space equipped with the inner product $\langle \cdot, \cdot \rangle$ and the induced norm $\| \cdot \|$. Let $\mathcal{Q} : \mathbb{R}^k \to \mathbb{R}^k$ be a continuous mapping, and let $\mathcal{K} \subset \mathbb{R}^k$ be a nonempty, closed, and convex set. We study the classical variational inequality problems (VIPs), which consists of finding a point $\vartheta^* \in \mathcal{K}$ such that:

$$\langle \mathcal{Q}(\vartheta^*), z - \vartheta^* \rangle \geq 0, \quad \forall z \in \mathcal{K}. \tag{1}$$

Inequality (1) represents the classical VIP, where the objective is to determine a point $\vartheta^* \in K$ such that the mapping $\mathcal{Q}$ forms a non-negative inner product with every feasible direction $z - \vartheta^*$. Geometrically, this condition characterizes equilibrium states and optimality conditions in constrained systems. VIPs have been extensively investigated due to their wide applicability in areas such as optimization, complementarity problems, saddle-point (min–max) formulations, Nash equilibrium models, and fixed-point theory [1]. This broad relevance has led to the development of various numerical methods, among which projection-based techniques play a central role (see, for instance [1–8]). By virtue of the projection theorem [1], a point $\vartheta^* \in \mathcal{K}$ is a solution of $VI(\mathcal{Q}, \mathcal{K})$, as given in (1), if and only if it satisfies the following fixed-point characterization for some $\eta > 0$:

$$\vartheta^* = \mathcal{P}_{\mathcal{K}}(\vartheta^* - \eta \mathcal{Q}(\vartheta^*)). \tag{2}$$

An important generalization of the VIP is its inverse counterpart associated with $VI(\mathcal{Q}, \mathcal{K})$. Let $\mathrm{Y} : \mathbb{R}^k \to \mathbb{R}^k$ be a single-valued mapping. Provided that the inverse relation $w = \mathrm{Y}^{-1}(z) = \mathcal{Q}(z)$ exists, the VIP can be reformulated as an inverse variational inequality problem (IVIP), denoted by IVIP$(\mathrm{Y}, \mathcal{K})$. This problem consists of finding $\mathrm{w}^* \in \mathbb{R}^k$ such that:

$$\mathrm{Y}(\mathrm{w}^*) \in \mathcal{K} \text{ and } \langle z - \mathrm{Y}(\mathrm{w}^*), \mathrm{w}^* \rangle \geq 0, \quad \forall z \in \mathcal{K}. \tag{3}$$

IVIPs arise in a variety of applications, such as economic equilibrium models [9] and traffic network analysis [10]. Despite their relevance, comparatively limited theoretical and computational methods have been developed for solving IVIP$(\mathrm{Y}, \mathcal{K})$ defined in (3). This problem can be equivalently expressed in terms of the following projection equation:

$$\mathrm{Y}(\mathrm{w}^*) = \mathcal{P}_{\mathcal{K}}\big[\mathrm{Y}(\mathrm{w}^*) - \eta \mathrm{w}^*\big], \tag{4}$$

where $\eta > 0$ is a fixed constant and $\mathcal{P}_{\mathcal{K}} : \mathbb{R}^k \to \mathcal{K}$ denotes the metric projection onto $\mathcal{K}$, defined by:

$$\mathcal{P}_{\mathcal{K}}(w) = \arg\min_{z \in \mathcal{K}} \|w - z\|, \quad w \in \mathbb{R}^k. \tag{5}$$

In [11], Zou et al. (2016) proposed a dynamical system, interpreted as a neural network model, for solving IVIP$(\mathrm{Y}, \mathcal{K})$ in (3). The approach is based on the following differential system:

$$\dot{w} = \sigma\Big[\mathcal{P}_{\mathcal{K}}\big(\mathrm{Y}(w) - \eta w\big) - \mathrm{Y}(w)\Big], \tag{6}$$

where $\dot{w} = \frac{dw}{dt}$, $\mathcal{P}_{\mathcal{K}}$ is defined in (5) and $\sigma > 0$ is a fixed parameter. He et al. [12] formulated the IVIP$(\mathrm{Y}, \mathcal{K})$ and developed a projection-based iterative algorithm for its solution, applying their approach to solve many equilibrium problems. IVIP$(\mathrm{Y}, \mathcal{K})$ has significant applications in engineering science, including transportation and telecommunication networks [13,14].

A number of studies have focused on extending IVIPs, leading to the development of inverse quasi-variational inequality problems (IQVIPs) [15–17]. The present work considers IQVIPs, which consist of finding a point $\mathrm{w}^* \in \mathbb{R}^k$ satisfying:

$$\mathrm{Y}(\mathrm{w}^*) \in \Phi(\mathrm{w}^*) \quad \text{and} \quad \langle \mathrm{w}^*, v - \mathrm{Y}(\mathrm{w}^*) \rangle \geq 0 \quad \forall v \in \Phi(\mathrm{w}^*), \tag{7}$$

where $\mathrm{Y} : \mathbb{R}^k \to \mathbb{R}^k$ denotes a single-valued operator and $\Phi : \mathbb{R}^k \to 2^{\mathbb{R}^k}$ is a set-valued mapping. Observe that if the constraint mapping is constant, i.e., $\Phi(w) = \mathcal{K}$ for all $w \in \mathbb{R}^k$, then, the problem reduces to the classical IVIP. First-order neurodynamic models have since been widely applied to VIPs due to their stability and parallel computational structure [18–21].

https://doi.org/10.3390/mca31030093

The concept of finite-time (FT) convergence, introduced in [22], has inspired the development of various dynamical models exhibiting this property (see [23,24]). In such models, the settling time depends on the initial state and may increase indefinitely as the initial deviation from equilibrium grows. However, in many practical applications such as robotics and vehicle-monitoring networks, precise knowledge of the initial state is often unavailable, making it difficult to determine the settling time in advance. To overcome this drawback, Polyakov in [25] introduced the notion of fixed-time (FXT) convergence, where convergence time is bounded by a constant not dependent of the initial state. This idea has since been further explored in several studies; see, for example [26–32].

FT and FXT convergence are two fundamentally distinct stability notions. In FT convergence, the settling time depends on the initial conditions and may increase as the initial state moves away from equilibrium. In contrast, FXT convergence guarantees a uniform upper bound on the settling time independent of initial conditions, offering stronger performance guarantees for real-time applications. Both FT and FXT principles have been successfully applied in a wide range of areas, including optimization problems [33–36], sparse optimization [37–41], multi-agent control [32], and variational inequality-related problems such as Mixed VIPs and equilibrium problems [26,27,42]. Also, some authors explored variational inclusion and fixed-point methods from both theoretical and computational viewpoints [43,44]. These works emphasize the importance of projection-type techniques in optimization and nonlinear analysis.

More recently, FT and FXT neurodynamic models with time-varying coefficients have been studied for optimization and variational inequality problems due to their improved convergence behavior and adaptive transient performance [45–47]. However, these existing studies mainly focus on classical optimization problems and standard VIs, and do not address IQVIPs involving state-dependent constraint mappings. For IQVIPs, Dey and Reich [16] proposed a nominal projected neurodynamic model with constant coefficients, while Van Tran and Le [48] developed FT and FXT neurodynamic systems for IQVIPs under constant-coefficient settings. However, their framework did not investigate robustness analysis under bounded disturbances. Motivated by these developments, the present work extends neurodynamic approaches for IQVIPs using FT and FXT dynamics with adaptive time-varying coefficients. In contrast to the existing constant-coefficient frameworks, the proposed models incorporate time-varying gains to improve flexibility, transient performance, and convergence regulation. Furthermore, FT and FXT convergence properties are established together with robustness analysis under bounded disturbances and a projection-based discretization framework.

To highlight practical relevance, a dedicated section on real-world applications and practical implications is included, where the proposed framework is connected to representative domains such as traffic equilibrium in intelligent transportation systems, resource allocation and congestion control in communication networks, distributed optimization in engineering systems, and coordination in multi-agent and robotic systems. This demonstrates the adaptability of the time-varying structure in dynamic environments and the advantage of FXT convergence for predictable performance in real-time implementations.

The following is a summary of this paper's main contributions:

- A unified framework of two different FT and FXT neurodynamic models with adaptive time-varying coefficients is developed for solving IQVIPs, extending existing constant-coefficient neurodynamic frameworks to a more flexible time-varying setting while bridging theoretical analysis and practical implementation.
- Novel projected TVCNDMs are proposed, exhibiting FT and FXT convergence behaviors with improved transient performance and enhanced adaptability.

- The equivalence between equilibrium points of a nominal dynamical model and solutions of IQVIPs is rigorously established, supported by appropriate analytical results.
- Lyapunov-based analysis is employed to guarantee existence, uniqueness, and global convergence of the proposed models under Lipschitz continuity and strong monotonicity assumptions, along with explicit settling-time estimates for FT and FXT convergence in the continuous-time setting.
- The robustness of the proposed models under bounded disturbances is analyzed, ensuring reliable performance in uncertain and dynamic environments.
- A projection-based discretization scheme is developed to obtain an implementable iterative algorithm. Numerical results demonstrate that all trajectories converge within a uniform bound, which is consistent with the fixed-time stability characteristics of the continuous-time model.
- The proposed framework is applicable to a variety of real-world problems, including traffic equilibrium, communication networks, distributed control systems, and multi-agent coordination.

The remainder of this paper is organized as follows: Section 2 presents the preliminaries, basic definitions, and the proposed nominal time-varying neurodynamic model for IQVIPs. Section 3 establishes the finite-time stability analysis of the proposed FT-TVCNDM. Section 4 investigates the fixed-time convergence properties of the FXT-TVCNDM. Robust fixed-time stability under bounded disturbances is analyzed in Section 5. Section 6 provides numerical experiments to validate the theoretical findings. Section 7 discusses real-world applications and practical implications of the proposed framework. Section 8 provides the results and discussion of the numerical experiments. Finally, concluding remarks and future research directions are presented in Section 9.

2. Preliminaries

In this part, we recall several fundamental definitions that will be utilized in the subsequent analysis.

Definition 1 ([49]). *The operator* $\Upsilon : \mathbb{R}^k \to \mathbb{R}^k$ *is said to be:*

(a) Monotone on $\mathbb{R}^k$*, if:*

$$\langle \Upsilon(w) - \Upsilon(v), w - v \rangle \geq 0, \quad \forall w, v \in \mathbb{R}^k.$$

(b) Strongly monotone on $\mathbb{R}^k$ *with modulus* $\beta > 0$*, if:*

$$\langle \Upsilon(w) - \Upsilon(v), w - v \rangle \geq \beta \|w - v\|^2, \quad \forall w, v \in \mathbb{R}^k.$$

(c) L-Lipschitz continuous on $\mathbb{R}^k$ *if* $\exists$ *a* $L \geq 0$*, such that:*

$$\|\Upsilon(w) - \Upsilon(v)\| \leq L\|w - v\| \quad \forall w, v \in \mathbb{R}^k.$$

It is worth noting that when $\mathcal{K}$ is nonempty, closed, and convex, $\mathcal{P}_{\mathcal{K}}(u)$ exists and is unique. Some useful properties of the projection operator are listed below.

Lemma 1 ([50]). *Let* $\mathcal{K}$ *be a nonempty, closed, convex set in* $\mathbb{R}^k$*. Let* $u, y \in \mathbb{R}^k$*. Then, one has*

1. $v = \mathcal{P}_{\mathcal{K}}(u) \iff \langle v - u, w - u \rangle \leq 0 \ \ \forall w \in \mathcal{K}$.
2. $\mathcal{P}_{\mathcal{K}}$ *is 1-Lipschitz continuous on* $\mathcal{K}$.

Lemma 2. *For any* $a, b, c \in \mathbb{R}^k$*, the following inequalities are satisfied:*

1. $\langle a, b \rangle \leq \|a\|\|b\|$.

2. *(Pythagoras identity), it holds that* $2\langle a-b, c-b\rangle = \|a-b\|^2 + \|c-b\|^2 - \|a-c\|^2$.

2.1. Lyapunov Stability Conditions

Consider the following time-varying model:

$$\dot{w} = \chi(t, w(t)), \qquad w(t_0) = w_0, \tag{8}$$

where $w : [t_0, +\infty) \to \mathbb{R}^k$, and $\chi : [t_0, +\infty) \times \mathbb{R}^k \to \mathbb{R}^k$ is continuous.

Definition 2 ([22]). *We say that* $\mathsf{w}^* \in \mathbb{R}^k$ *is an equilibrium point of* (8) *if:*

$$\chi(t, \mathsf{w}^*) = 0, \quad \forall\, t > t_0. \tag{9}$$

1. *Lyapunov stability: For any* $\mathcal{E} > 0$, *there exists* $\Sigma = \Sigma(\mathcal{E}, t_0)$ *such that:*

$$\|w_0 - \mathsf{w}^*\| < \Sigma \;\Rightarrow\; \|w(t) - \mathsf{w}^*\| < \mathcal{E}, \quad \forall\, t > t_0. \tag{10}$$

2. *Uniform stability: For any* $\mathcal{E} > 0$, *there exists* $\Sigma = \Sigma(\mathcal{E}) > 0$, *independent of* t_0, *such that* (10) *holds.*

Definition 3 ([51]). *From the model* (8), *we obtained an equilibrium point* w^* *of* (8) *which is said to be FT convergence if there exists a FT,* $\mathcal{T} : \mathbb{R}^k \setminus \{0\} \to (0, \infty)$ *(i.e.,* $\mathcal{T} < \infty$*) such that for all* $w(0) \in N \setminus \{0\}$*:*

$$\lim_{t \to \mathcal{T}} w(t) = 0 \quad \textit{and} \quad \mathcal{T} = \mathcal{T}(w(0)) < \infty.$$

Remark 1. *A solution* $w(t)$ *of model* (8) *exists on an interval containing* $t_0 = 0$ *if* χ *is continuous on its domain. Additionally, the uniqueness of the solution to* (8) *follows from the local Lipschitz continuity of* χ. *Any equilibrium point of* (8) *which is not at the origin can be translated to the origin by a suitable change in variables (see [52]). In particular, let* $\tilde{w}$ *be a nonzero equilibrium point of* (8) *and define* $z := w - \tilde{w}$. *Then, in terms of the new variable* u,

$$\dot{z} = \dot{w} = \mathcal{A}, \qquad z(0) = z_0 \in \mathbb{R}^k,$$

the origin $z = 0$ *becomes an equilibrium point, where* $\mathcal{A} := \chi(z + \tilde{w})$. *Hence, Definition* (3) *applies whether the model* $\dot{w} = \chi(w)$ *has its equilibrium point at the origin or not.*

Definition 4 ([25]). *The equilibrium point of* (8) *is said to be FXT-stable if it is FT-stable and there exists an upper bound* $\mathcal{T}_{\max} < \infty$ *such that:*

$$\sup_{w_0 \in \mathbb{R}^k} \mathcal{T}(w_0) \le \mathcal{T}_{\max}.$$

Lemma 3 ([45]). *Let there exist a continuously differentiable positive definite function* $\mathcal{L} : [t_0, +\infty) \times \mathbb{R}^k \to \mathbb{R}_+$ *satisfying:*

$$\dot{\mathcal{L}}(t, w(t)) \le -m_1 \phi_1(t) \mathcal{L}^{\vartheta_1}(t, w(t)) - m_2 \phi_2(t) \mathcal{L}^{\vartheta_2}(t, w(t)), \tag{11}$$

where $m_1 > 0$, $m_2 > 0$, $0 < \vartheta_1 < 1$, $\vartheta_2 > 1$ *are constants, and* $\dot{\mathcal{L}}(t, w) := \frac{\partial \mathcal{L}}{\partial t}(t, w) + \frac{\partial \mathcal{L}}{\partial w}(t, w)\dot{w}$. *Let* $\phi_1, \phi_2 : [t_0, +\infty) \to \mathbb{R}_{++}$ *be continuous. Define:*

$$\mathcal{F}_1(t) = \int_{t_0}^{t} \phi_1(z)\, dz, \qquad \mathcal{F}_2(t) = \int_{t_0}^{t} \phi_2(z)\, dz.$$

If $\frac{1}{m_2(\vartheta_2-1)} < \int_{t_0}^{+\infty} \phi_2(z)\,dz$ *and* $\mathcal{F}_1 \circ \mathcal{F}_2^{-1}\Big(\frac{1}{m_2(\vartheta_2-1)}\Big) + \frac{1}{m_1(1-\vartheta_1)} < \int_{t_0}^{+\infty} \phi_1(z)\,dz$, *then, there exists* $\mathcal{T} > t_0$ *such that* $\mathcal{L}(t, w(t)) \equiv 0$ *for all* $t \geq \mathcal{T}$. *Moreover:*

$$\mathcal{T} \leq \mathcal{F}_1^{-1}\left(\mathcal{F}_1 \circ \mathcal{F}_2^{-1}\left(\frac{1}{m_2(\vartheta_2 - 1)}\right) + \frac{1}{m_1(1-\vartheta_1)}\right). \tag{12}$$

2.2. A Nominal Time-Varying Neurodynamic Model for IQVIPs

In this section we first recall a nominal neurodynamic model proposed in [16] for IQVIPs (7) and a result regarding the existence and uniqueness of solutions of IQVIPs (7). We then present several auxiliary results that will be useful in the subsequent analysis. In particular, we establish key inequalities that play a crucial role in studying FT and FXT stability.

To solve the IQVIP (7), we consider the following nominal time-varying neurodynamic model (TVNDM):

$$\dot{w}(t) = -\phi(t)\Big(\Upsilon(w) - \mathcal{P}_{\Phi(w)}(\Upsilon(w) - \eta w)\Big), \tag{13}$$

where $\phi(t) > 0$ is a continuous time-dependent gain for all $t > 0$. For any closed convex set $\Phi(w) \subseteq \mathbb{R}^k$, the projection operator onto $\Phi(w)$ is denoted by:

$$\mathcal{P}_{\Phi(w)} : \mathbb{R}^k \to \Phi(w),$$

where $\mathcal{P}_{\Phi(w)}(x)$ represents the metric projection of $x \in \mathbb{R}^k$ onto the set $\Phi(w)$.

The proposed TVNDM (13) employs a time-varying gain function $\phi(t)$ to regulate the convergence behavior dynamically. The projection operator ensures that the generated trajectories remain consistent with the feasible constraint set associated with the IQVIP. Such a structure enhances adaptability and improves transient convergence performance in dynamic environments.

Lemma 4 ([16]). *An equilibrium of TVNDM* (13) *corresponds exactly to a solution of IQVIP* (7). *Then, solving IQVIP* (7) *is equivalent to finding* $\mathsf{w}^* \in \mathbb{R}^k$ *satisfying:*

$$\Upsilon(\mathsf{w}^*) = \mathcal{P}_{\Phi(\mathsf{w}^*)}[\Upsilon(\mathsf{w}^*) - \eta \mathsf{w}^*]. \tag{14}$$

We recall a result on existence and uniqueness of solutions to IQVIP (7). To analyze FT and FXT stability, we make the following assumption:

Assumption 1. *Let* $\Phi : \mathbb{R}^k \longrightarrow 2^{\mathbb{R}^k}$ *be a set-valued mapping with nonempty, closed, and convex values and* $\Upsilon : \mathbb{R}^k \to \mathbb{R}^k$ *be an L-Lipschitz continuous and* β*-strongly monotone single-valued mapping. Assume that there exists some* $\mu > 0$ *such that:*

$$\|\mathcal{P}_{\Phi(w_1)}(w) - \mathcal{P}_{\Phi(w_2)}(w)\| \leq \mu \|w_1 - w_2\|, \quad \forall w_1, w_2, w \in \mathbb{R}^k \tag{15}$$

and

$$\theta = \sqrt{L^2 + \eta^2 - 2\eta\beta} + \mu < \eta.$$

Lemma 5 ([16]). *Suppose Assumption 1 holds. Then,* $\mathsf{w}^* \in \mathbb{R}^k$ *be the unique solution of the IQVIP.*

Lemma 6 ([48]). *Suppose Assumption 1 holds. Assume that the solution set of IQVIP* (7) *is nonempty. Let* $\mathsf{w}^* \in \mathbb{R}^k$ *be a solution of the IQVIP* (7). *Since* $\beta > \theta$, *it follows that* $(\beta - \theta) > 0$, *which ensures the positivity of the coefficient used in the subsequent stability analysis. Then, the following statements hold:*

1.

$$\left\|\mathcal{P}_{\Phi(w)}(\Upsilon(w)-\eta w)-\mathcal{P}_{\Phi(\mathsf{w}^*)}(\Upsilon(\mathsf{w}^*)-\eta \mathsf{w}^*)\right\| \leq \theta\|w-\mathsf{w}^*\|, \qquad \forall w \in \mathbb{R}^k. \quad (16)$$

2.

$$0<(\beta-\theta)\|w-\mathsf{w}^*\| \leq \|\Upsilon(w)-\mathcal{P}_{\Phi(w)}(\Upsilon(w)-\eta w)\| \leq (L+\theta)\|w-\mathsf{w}^*\|, \quad \forall w \neq \mathsf{w}^*. \quad (17)$$

3.

$$\left\langle w-\mathsf{w}^*, \Upsilon(w)-\mathcal{P}_{\Phi(w)}(\Upsilon(w)-\eta w)\right\rangle \geq (\beta-\theta)\|w-\mathsf{w}^*\|^2>0, \quad \forall w \neq \mathsf{w}^*. \quad (18)$$

Lemma 7 ([48]). *Suppose Assumption 1 holds. Define the operator:*

$$\Pi(w) := \Upsilon(w)-\mathcal{P}_{\Phi(w)}(\Upsilon(w)-\eta w), \qquad w \in \mathbb{R}^k.$$

Then, Π is Lipschitz continuous with modulus $(2L+\eta+\mu)>0$.

Lemma 8. *Suppose Assumption 1 holds. Then, the TVNDM (13) has a unique equilibrium point, which is also the unique solution of IQVIP (7).*

Proof. By Lemma 4, every equilibrium point of the TVNDM (13) corresponds to a solution of the IQVIP (7). Furthermore, under Assumption 1, Lemma 5 guarantees that the IQVIP (7) admits a unique solution $w^* \in \mathbb{R}^k$. Hence, there exists a unique point satisfying $\Upsilon(w^*)=\mathcal{P}_{\Phi(w^*)}(\Upsilon(w^*)-\eta w^*)$. Moreover, from Lemma 6, the operator

$$\Pi(w) := \Upsilon(w)-\mathcal{P}_{\Phi(w)}(\Upsilon(w)-\eta w)$$

satisfies

$$\langle w-w^*, \Pi(w)\rangle \geq (\beta-\theta)\|w-w^*\|^2>0,$$

for all $w \neq w^*$. This implies that $\Pi(w)=0$ if and only if $w=w^*$. Therefore, the TVNDM (13) possesses a unique equilibrium point, which coincides with the unique solution of the IQVIP (7). The proof is complete. □

3. FT Stability Analysis for a Time-Varying Model

Before presenting the main results, we now establish the Lyapunov stability conditions for FT convergence of time-varying neurodynamic model.

Lemma 9. *Consider the dynamical model (8), which is locally Lipschitz in w and let $\mathsf{w}^* \in \mathbb{R}^k$ denote one of its equilibrium points. Suppose that $\exists$ a neighborhood Ω of w^* and a continuously differentiable function: $\mathcal{L}:[t_0,\infty)\times\mathbb{R}^k \to \mathbb{R}_+$ such that $\mathcal{L}(t,0)=0$, $V(t,w)>0\ \forall w \neq 0$. Suppose that along the trajectories of the model*

$$\dot{\mathcal{L}}(t,w(t)) \leq -\aleph\phi(t)(\mathcal{L}(t,w(t)))^{\alpha}, \quad (19)$$

for all $t \geq t_0$ and $w \in \mathcal{V}\setminus\{\mathsf{w}^*\}$, for some open neighborhood $\mathcal{V} \subseteq \Omega$ of w^*, where $\aleph>0$, $0<\alpha<1$, and $\phi(t):[t_0,\infty)\to\mathbb{R}_+$ is continuous. Suppose, further that:

$$\int_{t_0}^{+\infty}\phi(s)\,ds > \frac{\mathcal{L}(w(0))^{1-\alpha}}{\aleph(1-\alpha)}, \quad (20)$$

then, the equilibrium w^* is a FT stable equilibrium point of (8). Furthermore, the settling time $\mathcal{T}$ satisfies:

$$\mathcal{T}(w(0)) \leq H^{-1}\frac{\mathcal{L}(w(0))^{1-\alpha}}{\aleph(1-\alpha)}, \quad \forall w(0) \in \mathcal{V} \tag{21}$$

where $H(t) = \int_{t_0}^{t} \phi(s)\, ds$.

Proof. First, we see that H is strictly increasing since h is a positive. Let $w : [t_0, +\infty) \to \mathbb{R}^k$ be a solution of (8). Let $\mathcal{L} : [t_0, +\infty) \to \mathbb{R}_+$ be given by $\mathcal{L}(t) = \mathcal{L}(t, w(t))$. It follows from (19) that, for all $t \geq t_0$,

$$\dot{\mathcal{L}}(t) \leq -\aleph\phi(t)\mathcal{L}(t)^{\alpha}. \tag{22}$$

Now, we consider $T = \sup\{t_1 \geq t_0 : \mathcal{L}(t) > 0 \text{ for all } t \in [t_0, t_1]\}$. By (22), for all $t \in [t_0, T)$, $\mathcal{L}(t)^{-\alpha}\dot{\mathcal{L}}(t) \leq -\aleph\phi(t)$. For any $t_1 \in [t_0, T)$, integrating this inequality on $[t_0, t_1]$ yields:

$$\frac{\mathcal{L}(t_1)^{1-\alpha}}{\aleph(1-\alpha)} - \frac{\mathcal{L}(t_0)^{1-\alpha}}{\aleph(1-\alpha)} \leq -\phi(t_1).$$

By combining with $\alpha < 1$, $\mathcal{L}(t_0) \leq \mathcal{L}(t_1) > 0$, and $w \in \mathcal{V} \setminus \{\mathrm{w}^*\}$, for some open neighborhood $\mathcal{V} \subseteq \Omega$ of w^*, and (20),

$$H(t_1) \leq \frac{\mathcal{L}(t_0)^{1-\alpha}}{\aleph(1-\alpha)} - \frac{\mathcal{L}(t_1)^{1-\alpha}}{\aleph(1-\alpha)} < \frac{\mathcal{L}(w(0))^{1-\alpha}}{\aleph(1-\alpha)} < \int_{t_0}^{+\infty} \phi(s)\, ds.$$

where for all $w(0) \in \mathcal{V}$. Moreover, $\lim_{t\to\infty} H(t) = \int_{t_0}^{+\infty} \phi(s)\, ds,$; hence, $H(t_1) < \frac{\mathcal{L}(w(0))^{1-\alpha}}{\aleph(1-\alpha)} < \lim_{t\to\infty} H(t)$. As H is strictly increasing, $t_1 < H^{-1}\Big(\frac{\mathcal{L}(w(0))^{1-\alpha}}{\aleph(1-\alpha)}\Big) < +\infty$, which implies that:

$$T \leq H^{-1}\left(\frac{\mathcal{L}(w(0))^{1-\alpha}}{\aleph(1-\alpha)}\right) < +\infty. \tag{23}$$

Now, the definition of $\mathcal{T}$ and the continuity of $\mathcal{L}$ imply that $\mathcal{L}(T) = 0$. Since $\alpha > 0$, and $\dot{\mathcal{L}}(t) \leq -\aleph\phi(t)\mathcal{L}(t)^{\alpha} \leq 0$, we show that $\mathcal{L}$ is nonincreasing. Combining with the assumption that $\mathcal{L}$ is non-negative, we obtain that $\mathcal{L}(t) = 0$ for all $t \geq T$ and so, for all $t \geq T$, $\mathcal{L}(t, x(t)) = \mathcal{L}(t) = 0$. □

To study the FT stability of the IQVIP (7), a first-order FT-TVCNDM is constructed, whose equilibrium point corresponds to the solution of (7). Under appropriate parameter conditions, the proposed neurodynamic model is shown to be FT stable. Accordingly, the FT-TVCNDM associated with (7) is defined as follows:

$$\dot{w} = -\phi(t)\frac{\Upsilon(w) - \mathcal{P}_{\Phi(w)}(\Upsilon(w) - \eta w)}{\|\Upsilon(w) - \mathcal{P}_{\Phi(w)}(\Upsilon(w) - \eta w)\|^{\frac{\rho-2}{\rho-1}}}, \tag{24}$$

where $\rho > 2$ is a parameter and $\phi(t) : [t_0, +\infty) \to \mathbb{R}_{++}$ is continuous function.

It should be noted that for any $w \in \mathbb{R}^k$ satisfying $\Upsilon(w) - \mathcal{P}_{\Phi(w)}(\Upsilon(w) - \eta w) = 0$, the right-hand side of (24) remains well defined for all $\rho > 2$. In this case, the expression evaluates to zero. Indeed, we have:

$$\left\| \frac{\Upsilon(w) - \mathcal{P}_{\Phi(w)}(\Upsilon(w) - \eta w)}{\|\Upsilon(w) - \mathcal{P}_{\Phi(w)}(\Upsilon(w) - \eta w)\|^{\frac{\rho-2}{\rho-1}}} \right\| = \|\Upsilon(w) - \mathcal{P}_{\Phi(w)}(\Upsilon(w) - \eta w)\|^{\frac{1}{\rho-1}} = 0. \tag{25}$$

The following result shows that the equilibrium points of (24) coincide with TVNDM (13).

Proposition 1. *If* $\mathsf{w}^* \in \mathbb{R}^k$ *is an equilibrium point of* (24) $\iff$ *it is also an equilibrium point of TVNDM* (13).

Proof. A necessary and sufficient condition for $\mathsf{w}^* \in \mathbb{R}^k$ to be an equilibrium point of FT-TVCNDM (24) is that:

$$\begin{aligned}\phi(t)\frac{\Upsilon(\mathsf{w}^*)-\mathcal{P}_{\Phi(w)}(\Upsilon(\mathsf{w}^*)-\eta\mathsf{w}^*)}{\|\Upsilon(\mathsf{w}^*)-\mathcal{P}_{\Phi(w)}(\Upsilon(\mathsf{w}^*)-\eta\mathsf{w}^*)\|^{\frac{\rho-2}{\rho-1}}}=0 &\iff \frac{\|\Upsilon(\mathsf{w}^*)-\mathcal{P}_{\Phi(w)}(\Upsilon(\mathsf{w}^*)-\eta\mathsf{w}^*)\|}{\|\Upsilon(\mathsf{w}^*)-\mathcal{P}_{\Phi(w)}(\Upsilon(\mathsf{w}^*)-\eta\mathsf{w}^*)\|^{\frac{\rho-2}{\rho-1}}}=0\\ &\iff \left(\Upsilon(\mathsf{w}^*)-\mathcal{P}_{\Phi(w)}(\Upsilon(\mathsf{w}^*)-\eta\mathsf{w}^*)\right)^{1-\frac{\rho-2}{\rho-1}}=0.\end{aligned} \tag{26}$$

From $1-\frac{\rho-2}{\rho-1}=\frac{1}{\rho-1}>0 \quad \forall \rho>2$, we conclude that Equation (26) holds $\iff$

$$\Upsilon(\mathsf{w}^*)-\mathcal{P}_{\Phi(w)}(\Upsilon(\mathsf{w}^*)-\eta\mathsf{w}^*)=0, \tag{27}$$

or

$$\Upsilon(\mathsf{w}^*)=\mathcal{P}_{\Phi(w)}(\Upsilon(\mathsf{w}^*)-\eta\mathsf{w}^*). \tag{28}$$

Hence, w^* is an equilibrium point of TVNDM (13). □

The result below is an immediate consequence of Lemma 8 together with Proposition 1.

Corollary 1. *Suppose* w^* *is a solution of IQVIP* (7) $\iff$ *it is an equilibrium point of FT-TVCNDM*(24).

Proof. It is a direct consequence of Lemma 8 together with Proposition 1. □

The following result presents the FT stability analysis of the FT-TVCNDM (24). Many existing FT neurodynamic frameworks for variational inequality-related problems have been developed using constant coefficients [22,48]. Different from these approaches, the proposed FT-TVCNDM employs adaptive time-varying coefficients, providing greater flexibility and allowing for finite-time convergence analysis under more general conditions.

Theorem 1. *Suppose Assumption 1 holds. Then,* $\mathsf{w}^* \in \mathbb{R}^k$*, being the solution* (7)*, is an FT-stable equilibrium point of FT-TVCNDM* (24) *with a settling time*

$$\mathcal{T}(w(0)) \leq \mathcal{T}_{\max} = H^{-1}\frac{(w(0)-\mathsf{w}^*)^{2(1-\alpha)}}{2^{1-\alpha}\aleph(1-\alpha)} \tag{29}$$

for constants $\aleph, \mathcal{T} > 0$ *and* $\alpha \in (0.5, 1)$*, where* $H(t) = \int_{t_0}^{t} \phi(s)\, ds$.

Proof. We take Lyapunov function $\mathcal{L} : \mathbb{R}^k \to \mathbb{R}$ as follows:

$$\mathcal{L}(w) := \frac{1}{2}\|w-\mathsf{w}^*\|^2. \tag{30}$$

Now, we differentiate (30) to obtain:

$$\dot{\mathcal{L}}(w) = \langle w-\mathsf{w}^*, \dot{w}\rangle.$$

Thus, from any $w(0) \in \mathbb{R}^k \setminus \{\mathsf{w}^*\}$, with w^* being the unique solution in $\mathrm{Zer}(\Pi(\cdot))$ defined by $\Pi(\cdot) = \Upsilon(\cdot) - \mathcal{P}_{\Phi(\cdot)}(\Upsilon(\cdot) - \eta(\cdot))$, we have:

$$\dot{\mathcal{L}} = -\left\langle w - \mathsf{w}^*, \phi(t) \frac{\Upsilon(w) - \mathcal{P}_{\Phi(w)}(\Upsilon(w) - \eta w)}{\|\Upsilon(w) - \mathcal{P}_{\Phi(w)}(\Upsilon(w) - \eta w)\|^{\frac{\rho-2}{\rho-1}}} \right\rangle$$
$$= -\phi(t) \frac{\langle w - \mathsf{w}^*, \Upsilon(w) - \mathcal{P}_{\Phi(w)}(\Upsilon(w) - \eta w)\rangle}{\|\Upsilon(w) - \mathcal{P}_{\Phi(w)}(\Upsilon(w) - \eta w)\|^{\frac{\rho-2}{\rho-1}}}. \tag{31}$$

By Part (3) of Lemma 6, it follows that:

$$\dot{\mathcal{L}} \leq -\phi(t)(\beta - \theta) \frac{\|w - \mathsf{w}^*\|^2}{\|\Upsilon(w) - \mathcal{P}_{\Phi(w)}(\Upsilon(w) - \eta w)\|^{\frac{\rho-2}{\rho-1}}} \tag{32}$$

By Part (2) of Lemma 6, we obtain:

$$\dot{\mathcal{L}} \leq -\phi(t)(\beta - \theta)(\beta - \theta)^{\frac{\rho-2}{\rho-1}} \frac{\|w - \mathsf{w}^*\|^2}{\|w - \mathsf{w}^*\|^{\frac{\rho-2}{\rho-1}}}$$
$$= -\phi(t)(\beta - \theta)^{\frac{1}{\rho-1}} \|w - \mathsf{w}^*\|^{\frac{\rho}{\rho-1}}. \tag{33}$$

Setting $N := (\beta - \theta)^{\frac{1}{\rho-1}}$, where $\theta = \sqrt{(L^2 + \eta^2 - 2\eta\beta)} + \mu$, condition $\theta < \beta$ implies that $N > 0$, Equations (33) and (30) can be written as follows:

$$\dot{\mathcal{L}} \leq -N\phi(t)\|w - \mathsf{w}^*\|^{\frac{\rho}{\rho-1}}$$
$$\leq -N\phi(t)\, 2^{\frac{\rho}{2(\rho-1)}} \left(\frac{1}{2}\|w - \mathsf{w}^*\|^2\right)^{\frac{\rho}{2}\frac{1}{\rho-1}} \tag{34}$$
$$= -N\phi(t)\, 2^{\frac{\rho}{2(\rho-1)}} \mathcal{L}^{\frac{\rho}{2}\frac{1}{\rho-1}}. \tag{35}$$

Applying Lemma 9 and observing that

$$0.5 < \alpha := \frac{\rho}{2}\frac{1}{\rho - 1} < 1 \quad \text{for all } \rho > 2, \text{ with } \aleph := N \cdot 2^{\alpha} > 0,$$

the conclusion follows. The proof is complete. □

Remark 2. *By discretizing the continuous-time model (24) via the forward Euler method, we arrive at the following discrete scheme:*

$$w_{k+1} = w_k - h_k\, \Theta(w_k, t)\Big(\Upsilon(w_k) - \mathcal{P}_{\Phi(w)}(\Upsilon(w_k) - \eta w_k)\Big), \tag{36}$$

where $h_k > 0$ denotes the iteration-dependent step size, i.e., $h_k = h(k) > 0$ and initialize $w_0 \in \mathbb{R}^k$. The scaling factor $\Theta(w_k, t)$ is defined as follows:

$$\Theta(w_k, t) = \frac{\phi(t)}{\Big\|\Upsilon(w_k) - \mathcal{P}_{\Phi(w)}(\Upsilon(w_k) - \eta w_k)\Big\|^{\frac{\rho-2}{\rho-1}}},$$

where $\rho > 2$ and $\phi(t) : [t_0, +\infty) \to \mathbb{R}_{++}$ is continuous. For $k = 0, 1, 2, \ldots$ This discrete scheme provides an implementable iterative form of the proposed continuous-time model with a variable step size.

4. FXT Stability Analysis

This section analyzes the FXT stability of solutions of IQVIPs (7). We will introduce another projection TVCNDM for the problem (7). Next, we characterize the solutions of IQVIPs through equilibrium points of the proposed dynamical model. Finally, we establish the FXT convergence of the proposed TVCNDM.

4.1. The FXT-TVCNDM for IQVIPs

Inspired by research on continuous-time neurodynamic optimization methods for FXT convergence, we propose the following FXT-TVCNDM:

$$\dot{w} = -\theta(w,t)(\Upsilon(w) - \mathcal{P}_{\Phi(w)}(\Upsilon(w) - \eta w)), \tag{37}$$

where

$$\theta(w,t) := \begin{cases} \dfrac{\phi_1(t)}{\|\Upsilon(w) - \mathcal{P}_{\Phi(w)}(\Upsilon(w) - \eta w)\|^{1-\lambda_1}} \\ \quad + \dfrac{\phi_1(t)}{\|\Upsilon(w) - \mathcal{P}_{\Phi(w)}(\Upsilon(w) - \eta w)\|^{1-\lambda_2}}, \text{ if } w \in \mathbb{R}^k \setminus \mathrm{Zer}(\Pi), \\ 0 \quad \text{otherwise,} \end{cases} \tag{38}$$

$0 < \lambda_1 < 1$, $\lambda_2 > 1$ $\Pi(\cdot) = \mathcal{P}_{\Phi(w)}(\Upsilon(\cdot) - \eta(\cdot)) - \Upsilon(\cdot)$. $\phi_1(t), \phi_2(t) : [t_0, +\infty) \to \mathbb{R}_{++}$ are continuous functions. The FXT-TVCNDM (37) allows for greater flexibility through its time-varying coefficients. Moreover, note that FXT-TVCNDM (37) can be written in an equivalent form as follows:

$$\begin{aligned} \dot{w} = &-\phi_1(t)\kappa(w)\left\|\Upsilon(w) - \mathcal{P}_{\Phi(w)}(\Upsilon(w) - \eta w)\right\|^{\lambda_1} \\ &\times \left(1 + \frac{\phi_2(t)}{\phi_1(t)}\left\|\Upsilon(w) - \mathcal{P}_{\Phi(w)}(\Upsilon(w) - \eta w)\right\|^{\lambda_2 - \lambda_1}\right). \end{aligned} \tag{39}$$

where

$$\kappa(w) := \frac{\Upsilon(w) - \mathcal{P}_{\Phi(w)}(\Upsilon(w) - \eta w)}{\|\Upsilon(w) - \mathcal{P}_{\Phi(w)}(\Upsilon(w) - \eta w)\|}.$$

Remark 3. *1. In the FXT-TVCNDM (37), the term $-\kappa(w)$ can be interpreted as the search direction, while*

$$\begin{aligned} \eta_t := &-\phi_1(t)\left\|\Upsilon(w) - \mathcal{P}_{\Phi(w)}(\Upsilon(w) - \eta w)\right\|^{\lambda_1} \\ &\times \left(1 + \frac{\phi_2(t)}{\phi_1(t)}\left\|\Upsilon(w) - \mathcal{P}_{\Phi(w)}(\Upsilon(w) - \eta w)\right\|^{\lambda_2 - \lambda_1}\right) \end{aligned}$$

represents the stepsize at the current iterate $w = w(t)$. Once the functions $\phi_1(t), \phi_2(t)$ and λ_1, λ_2 are specified, the stepsize η_t is automatically updated with respect to t. Therefore, FXT-TVCNDM (37) may also be viewed as an FXT-TVCNDM with a self-adaptive dynamical step size.

2. By taking $\phi_2(t) = 1$, FXT-TVCNDM (37) is reduced to:

$$\begin{aligned} \dot{w} = &-\phi_1(t)\kappa(w)\left\|\Upsilon(w) - \mathcal{P}_{\Phi(w)}(\Upsilon(w) - \eta w)\right\|^{\lambda_1} \\ &\times \left(1 + \frac{1}{\phi_1(t)}\left\|\Upsilon(w) - \mathcal{P}_{\Phi(w)}(\Upsilon(w) - \eta w)\right\|^{\lambda_2 - \lambda_1}\right). \end{aligned}$$

3. *If $\phi_2(t) = 0$ and $\phi_1(t) = \sigma$ is a constant function, then, the proposed FXT-TVCNDM (37) reduces to:*

$$\dot{w}(t) = -\sigma\Big(\Upsilon(w) - \mathcal{P}_{\Phi(w)}\big(\Upsilon(w) - \eta w\big)\Big), \tag{40}$$

where $\sigma > 0$ is a constant. This reduced model was studied in [16] for solving IQVIP (7) under a constant-coefficient framework. Therefore, the proposed FXT-TVCNDM (37) can be regarded as a generalized time-varying extension of the constant-coefficient neurodynamic model introduced in [16].

The next result establishes the equivalence between the equilibrium points of the proposed FXT neurodynamic model and those of the nominal TVNDM (13).

Proposition 2. *A point $\mathsf{w}^* \in \mathbb{R}^k$ is an equilibrium point of model (37) if and only if it is an equilibrium point of TVNDM (13).*

Proof. The conclusion follows from the definition of the gain function $\theta(\cdot, t)$ in (38). Indeed,

$$\theta(\mathsf{w}^*, t) = 0 \quad \Longleftrightarrow \quad \Upsilon(\mathsf{w}^*) = \mathcal{P}_{\Phi(w)}(\Upsilon(\mathsf{w}^*) - \eta \mathsf{w}^*),$$

which coincides with the equilibrium condition of TVNDM (13). □

Combining Proposition 2 with Lemma 4, we obtain the following characterization of solutions of the IQVIP (7).

Corollary 2. *Suppose Assumption 1 holds. Then, w^* solves the IQVIP (7) if and only if it is an equilibrium point of the FXT-TVCNDM (37).*

Proof. The statement follows immediately from Propositions 2 and Lemma 4. □

The following lemma gives conditions so that solutions of the given neurodynamic model exist and are uniquely determined in the classical sense.

Lemma 10 ([26])**.** *Let $\Pi : \mathbb{R}^k \to \mathbb{R}^k$ be a locally Lipschitz continuous vector field satisfying:*

$$\Pi(\tilde{w}) = 0, \qquad \langle w - \tilde{w}, \Pi(w)\rangle > 0, \quad \forall w \in \mathbb{R}^k \setminus \{\tilde{w}\}.$$

Then, the associated dynamical system admits a unique classical solution.

We now show that solutions to the FXT-TVCNDM (37) exist and are uniquely determined. The following result guarantees the well-posedness of the proposed FXT-TVCNDM.

Proposition 3. *Suppose Assumption 1 holds. Then, the model (37) has a unique solution in a classical sense.*

Proof. By Lemma 5, IQVIP (7) has a unique solution. It follows that the set $\mathrm{Zer}(\Pi)$ is a singleton; here, $\Pi(w) \equiv \Upsilon(w) - \mathcal{P}_{\Phi(w)}(\Upsilon(w) - \eta w)$. Thus, the model (13) has a unique equilibrium point $\overline{w} = \mathsf{w}^*$. By Lemma 6, Part (3), the vector field $\Pi(w) \equiv \Upsilon(w) - \mathcal{P}_{\Phi(w)}(\Upsilon(w) - \eta w)$ satisfies the following property:

$$\langle w - \overline{w}, \Pi(w)\rangle > 0$$

for all $w \in \mathbb{R}^k \setminus \{\overline{w}\}$, where $\{\overline{w}\} = \mathrm{Zer}(\Pi)$. Also, by Lemma 7, the operator $\Pi(\cdot) = \mathcal{P}_{\Phi(\cdot)}(\Upsilon(\cdot) - \eta(\cdot)) - \Upsilon(\cdot)$ is Lipschitz continuous. This implies Lipschitz conti-

nuity on $\mathbb{R}^k$ of the vector field on the right-hand side of (13). Finally, the conclusion follows from Lemma 10. □

4.2. FXT Convergence

The following theorem presents the main result of this section. Suppose $\mathsf{w}^* \in \mathbb{R}^k$ denote the unique equilibrium of FXT-TVCNDM (37). Then, the equilibrium w^*, which coincides with the solution of the IQVIP (7), is FXT-stable.

Theorem 2. *Suppose Assumption 1 is satisfied. Furthermore, suppose that* $\frac{1}{m_2(\vartheta_2-1)} < \int_{t_0}^{+\infty} \phi_2(z)\,dz$ *and* $\mathcal{F}_1 \circ \mathcal{F}_2^{-1}\left(\frac{1}{m_2(\vartheta_2-1)}\right) + \frac{1}{m_1(1-\vartheta_1)} < \int_{t_0}^{+\infty} \phi_1(z)\,dz$, *where* $\vartheta_1 = \frac{1+\lambda_1}{2}$, $\vartheta_2 = \frac{1+\lambda_2}{2}$, $m_1 = 2^{\vartheta_1}\frac{(\beta-\theta)}{(L+\theta)^{1-\lambda_1}}$, *and* $m_2 = 2^{\vartheta_2}(\beta-\theta)^{\lambda_2}$ *for some* $\aleph \in (0,1)$ *with*

$$\mathcal{F}_1(t) = \int_0^t \phi_1(z)\,dz, \qquad \mathcal{F}_2(t) = \int_0^t \phi_2(z)\,dz,$$

then, the state $w(t)$ *of* (37) *converges to* w^* *with settling time described as follows:*

$$\mathcal{T} \leq \mathcal{F}_1^{-1}\left(\mathcal{F}_1 \circ \mathcal{F}_2^{-1}\left(\frac{1}{m_2(\vartheta_2-1)}\right) + \frac{1}{m_1(1-\vartheta_1)}\right). \tag{41}$$

Proof. By Proposition 3, the FXT-TVCNDM (37) admits a uniquely determined solution for all forward times. We next take the Lyapunov function:

$$\mathcal{L}(t, w(t)) = \frac{1}{2}\|w - \mathsf{w}^*\|^2. \tag{42}$$

Then, $\mathcal{L}(w) = 0 \iff w = \mathsf{w}^*$ and $\mathcal{L}(w) \to \infty$ as $\|w\| \to \infty$. Taking the time derivative of (42) along the trajectories of (37), we examine the Lyapunov function (42) for any $w(0) \in \mathbb{R}^k \setminus \{\mathsf{w}^*\}$. Observing that w^* is unique element of $\mathrm{Zer}\Big(\mathrm{Y}(\cdot) - \mathcal{P}_{\Phi(\cdot)}\big(\mathrm{Y}(\cdot) - \eta\,\mathrm{id}(\cdot)\big)\Big)$, it follows that:

$$\begin{aligned}
\dot{\mathcal{L}}(t,w) &= \langle w - \mathsf{w}^*, \dot{w}\rangle \\
&= -\phi_1(t)\frac{1}{\|\mathrm{Y}(w) - \mathcal{P}_{\Phi(w)}(\mathrm{Y}(w) - \eta w)\|^{1-\lambda_1}}\langle w - \mathsf{w}^*, \mathrm{Y}(w) - \mathcal{P}_{\Phi(w)}(\mathrm{Y}(w) - \eta w)\rangle \\
&+ \phi_2(t)\frac{1}{\|\mathrm{Y}(w) - \mathcal{P}_{\Phi(w)}(\mathrm{Y}(w) - \eta w)\|^{1-\lambda_2}}\langle w - \mathsf{w}^*, \mathrm{Y}(w) - \mathcal{P}_{\Phi(w)}(\mathrm{Y}(w) - \eta w)\rangle.
\end{aligned}$$

From Lemma 6, we obtain:

$$\langle w - \mathsf{w}^*, \mathrm{Y}(w) - \mathcal{P}_{\Phi(w)}(\mathrm{Y}(w) - \eta w)\rangle \geq (\beta-\theta)\|w - \mathsf{w}^*\|^2$$

and

$$(\beta-\theta)\|w - \mathsf{w}^*\| \leq \|\mathrm{Y}(w) - \mathcal{P}_{\Phi(w)}(\mathrm{Y}(w) - \eta w)\| \leq (L+\theta)\|w - \mathsf{w}^*\|.$$

Thus,

$$\begin{aligned}
\dot{\mathcal{L}}(t,w) &\leq -(\beta-\theta)\phi_1(t)\frac{\|w - \mathsf{w}^*\|^2}{(L+\theta)^{1-\lambda_1}\|w - \mathsf{w}^*\|^{1-\lambda_1}} \\
&\quad - (\beta-\theta)\phi_2(t)\frac{\|w - \mathsf{w}^*\|^2}{(\beta-\theta)^{1-\lambda_2}\|w - \mathsf{w}^*\|^{1-\lambda_2}} \qquad (43) \\
&= -\frac{(\beta-\theta)}{(L+\theta)^{1-\lambda_1}}\phi_1(t)\|w - \mathsf{w}^*\|^{1+\lambda_1} - (\beta-\theta)^{\lambda_2}\phi_2(t)\|w - \mathsf{w}^*\|^{1+\lambda_2}. \qquad (44)
\end{aligned}$$

Therefore, from Equations (42) and (43), we obtain:

$$\dot{\mathcal{L}}(t, w(t)) \leq -2^{\frac{1+\lambda_1}{2}} \frac{(\beta-\theta)}{(L+\theta)^{1-\lambda_1}} \phi_1(t) \mathcal{L}^{\frac{1+\lambda_1}{2}} - 2^{\frac{1+\lambda_2}{2}} (\beta-\theta)^{\lambda_2} \phi_2(t) \mathcal{L}^{\frac{1+\lambda_2}{2}}. \tag{45}$$

Let $\vartheta_1 = \frac{1+\lambda_1}{2}$, $\vartheta_2 = \frac{1+\lambda_2}{2}$, $m_1 = 2^{\vartheta_1} \frac{(\beta-\theta)}{(L+\theta)^{1-\lambda_1}}$, and $m_2 = 2^{\vartheta_2}(\beta-\theta)^{\lambda_2}$. Then, inequality (45) becomes:

$$\dot{\mathcal{L}} \leq -m_1 \phi_1(t) \mathcal{L}^{\vartheta_1} - m_2 \phi_2(t) \mathcal{L}^{\vartheta_2}.$$

Applying Lemma 3 with $\mathcal{F}_1(t) = \int_{t_0}^{t} \phi_1(z)\, dz$, $\mathcal{F}_2(t) = \int_{t_0}^{t} \phi_2(z)\, dz$, the trajectory $w(t)$ converges to w^* in fixed time, and the settling time satisfies:

$$\mathcal{T} \leq \mathcal{F}_1^{-1}\left(\mathcal{F}_1 \circ \mathcal{F}_2^{-1}\left(\frac{1}{m_2(\vartheta_2 - 1)}\right) + \frac{1}{m_1(1-\vartheta_1)}\right).$$

□

We now present several representative cases of the model (37), obtained through different choices of time-varying coefficient functions. These selections lead to various explicit expressions for the corresponding settling-time upper bounds.

Corollary 3. *Let Assumption (1) hold. Define* $\vartheta_1 = \frac{1+\lambda_1}{2}$, $\vartheta_2 = \frac{1+\lambda_2}{2}$, $m_1 = 2^{\vartheta_1} \frac{(\beta-\theta)}{(L+\theta)^{1-\lambda_1}}$, *and* $m_2 = 2^{\vartheta_2}(\beta-\theta)^{\lambda_2}$. *where* $\varpi_0 > 0$, $\varrho_0 > 0$, *and* $\tau > 0$.

1. *If one selects* $\phi_1(t) = \varpi_0$ *and* $\phi_2(t) = \varrho_0$ *in FXT-TVCNDM (37), then, the state* $w(t)$ *converges to* w^* *in the frequency domain, with settling time bounded by:*

$$T \leq \frac{1}{\varpi_0 m_1(1-\vartheta_1)} + \frac{1}{\varrho_0 m_2(\vartheta_2 - 1)}. \tag{46}$$

2. *If one selects* $\phi_1(t) = \frac{\varpi_0}{t+\tau}$ *and* $\phi_2(t) = \frac{\varrho_0}{t+\tau}$ *in FXT-TVCNDM (37), then,* $w(t)$ *converges to* w^* *in the frequency domain, with settling time bounded by:*

$$T \leq \tau \exp\left(\frac{1}{\varpi_0 m_1(1-\vartheta_1)} + \frac{1}{\varrho_0 m_2(\vartheta_2 - 1)}\right) - \tau. \tag{47}$$

3. *If one selects* $\phi_1(t) = \varpi_0$ *and* $\phi_2(t) = \frac{\varrho_0}{t+\tau}$ *in FXT-TVCNDM (37), then,* $w(t)$ *converges to* w^* *in the frequency domain, with settling time bounded by:*

$$T \leq \tau \exp\left(\frac{1}{\varrho_0 m_2(\vartheta_2 - 1)}\right) + \frac{1}{\varpi_0 m_1(1-\vartheta_1)} - \tau. \tag{48}$$

4. *If one selects* $\phi_1(t) = \frac{\varpi_0}{(t+\tau)^{\alpha_1}}$ *and* $\phi_2(t) = \frac{\varrho_0}{(t+\tau)^{\alpha_2}}$, *where* $\alpha_1 \neq 1$ *and* $\alpha_2 \neq 1$, *such that:*

$$\alpha = \frac{1-\alpha_2}{\varrho_0 m_2(\vartheta_2 - 1)} + \tau^{1-\alpha_2} > 0, \quad \text{and} \quad \alpha^{\frac{1-\alpha_1}{1-\alpha_2}} + \frac{1-\alpha_1}{\varpi_0 m_1(1-\vartheta_1)} > 0,$$

then, $w(t)$ *converges to* w^* *in the frequency domain, with settling time bounded by:*

$$T \leq \left(\alpha^{\frac{1-\alpha_1}{1-\alpha_2}} + \frac{1-\alpha_1}{\varpi_0 m_1(1-\vartheta_1)}\right)^{\frac{1}{1-\alpha_1}} - \tau. \tag{49}$$

As highlighted in Corollary 3, the derived settling-time bounds depend on the exponents λ_1 and λ_2, the operator parameters θ, β, and the Lipschitz constant L, along with the step size η and the time-varying gain functions $\phi_1(t)$ and $\phi_2(t)$. Therefore, for fixed values

of λ_1, λ_2, θ, β, L, and η, the convergence-time bound can be flexibly controlled through an appropriate selection of the time-varying coefficients $\phi_1(t)$ and $\phi_2(t)$.

5. Robust FXT Analysis

In this subsection, we investigate the robustness of the proposed FXT converging FXT-TVCNDM when it is subject to an external disturbance term $\mathcal{D}: \mathbb{R}^k \to \mathbb{R}^k$. Specifically, we consider the scenario where FXT convergence remains valid when FXT-TVCNDM (37) is exposed to interference:

$$\begin{aligned}\dot{w} = &-\left(\frac{\phi_1(t)}{\left\|\mathrm{Y}(w)-\mathcal{P}_{\Phi(w)}(\mathrm{Y}(w)-\eta w)\right\|^{1-\lambda_1}}+\frac{\phi_2(t)}{\left\|\mathrm{Y}(w)-\mathcal{P}_{\Phi(w)}(\mathrm{Y}(w)-\eta w)\right\|^{1-\lambda_2}}\right)\\ &\times\left(\mathrm{Y}(w)-\mathcal{P}_{\Phi(w)}(\mathrm{Y}(w)-\eta w)\right)+\mathcal{D}(w).\end{aligned} \tag{50}$$

where $\mathcal{D}(w)$ represents the interference affecting FXT-TVCNDM (37).

Assumption 2. *There exists a constant $q > 0$ such that for any $w \neq \mathrm{w}^* \in \mathbb{R}^k$,*

$$\|\mathcal{D}(w)\| < q\|w - \mathrm{w}^*\|.$$

It follows from Assumption 2 that w^* is an equilibrium point of model (50). The following result shows that the FXT convergent model (50) is robust with respect to external disturbances.

Theorem 3. *Let Assumption (1) hold. Suppose further that:*

$$\min\left\{\frac{(\beta-\theta)}{(L+\theta)^{1-\lambda_1}}\phi_1(t),\ (\beta-\theta)^{\lambda_2}\phi_2(t)\right\} > q,\ \frac{1}{m_2(\vartheta_2-1)} < \int_{t_0}^{+\infty}\phi_2(z)\,dz,$$

and $\mathcal{F}_1 \circ \mathcal{F}_2^{-1}\left(\frac{1}{m_2(\vartheta_2-1)}\right)+\frac{1}{m_1(1-\vartheta_1)} < \int_{t_0}^{+\infty}\phi_1(z)\,dz$, where $\vartheta_i = \frac{1+\lambda_i}{2}$, $i = 1,2$, $m_1 = 2^{\vartheta_1}\frac{(\beta-\theta)}{(L+\theta)^{1-\lambda_1}}$, and $m_2 = 2^{\vartheta_2}(\beta-\theta)^{\lambda_2}$ for some $\aleph \in (0,1)$ with

$$\mathcal{F}_1(t) = \int_0^t\left(\frac{(\beta-\theta)}{(L+\theta)^{1-\lambda_1}}\phi_1(z)-q\right)dz, \mathcal{F}_2(t) = \int_0^t\left((\beta-\theta)^{\lambda_2}\phi_2(z)-q\right)dz.$$

Under Assumption 2, the trajectory $w(t)$ of model (50) converges to w^* in fixed time.

Proof. Consider the Lyapunov function introduced in (42). Taking its time derivative and using Assumption 2, we obtain:

$$\begin{aligned}\dot{\mathcal{L}}(t,w) &= \langle w-\mathrm{w}^*, \dot{w}\rangle\\ &= -\phi_1(t)\frac{1}{\left\|\mathrm{Y}(w)-\mathcal{P}_{\Phi(w)}(\mathrm{Y}(w)-\eta w)\right\|^{1-\lambda_1}}\langle w-\mathrm{w}^*, \mathrm{Y}(w)-\mathcal{P}_{\Phi(w)}(\mathrm{Y}(w)-\eta w)\rangle\\ &\quad+\phi_2(t)\frac{1}{\left\|\mathrm{Y}(w)-\mathcal{P}_{\Phi(w)}(\mathrm{Y}(w)-\eta w)\right\|^{1-\lambda_2}}\langle w-\mathrm{w}^*, \mathrm{Y}(w)-\mathcal{P}_{\Phi(w)}(\mathrm{Y}(w)-\eta w)\rangle\\ &\quad+q\|w-\mathrm{w}^*\|^2.\end{aligned} \tag{51}$$

From Lemma 6, we obtain:

$$\langle w-\mathrm{w}^*, \mathrm{Y}(w)-\mathcal{P}_{\Phi(w)}(\mathrm{Y}(w)-\eta w)\rangle \geq (\beta-\theta)\|w-\mathrm{w}^*\|^2$$

and

$$(\beta-\theta)\|w-\mathsf{w}^*\| \le \|\Upsilon(w)-\mathcal{P}_{\Phi(w)}(\Upsilon(w)-\eta w)\| \le (L+\theta)\|w-\mathsf{w}^*\|.$$

Thus,

$$\begin{aligned}\dot{\mathcal{L}}(t,w(t)) \le & -(\beta-\theta)\phi_1(t)\frac{\|w-\mathsf{w}^*\|^2}{(L+\theta)^{1-\lambda_1}\|w-\mathsf{w}^*\|^{1-\lambda_1}} \\ & -(\beta-\theta)\phi_2(t)\frac{\|w-\mathsf{w}^*\|^2}{(\beta-\theta)^{1-\lambda_2}\|w-\mathsf{w}^*\|^{1-\lambda_2}} \\ & +q\|w-\mathsf{w}^*\|^2. \\ = & -\frac{(\beta-\theta)}{(L+\theta)^{1-\lambda_1}}\phi_1(t)\|w-\mathsf{w}^*\|^{1+\lambda_1}-(\beta-\theta)^{\lambda_2}\phi_2(t)\|w-\mathsf{w}^*\|^{1+\lambda_2} \\ & +q\|w-\mathsf{w}^*\|^2.\end{aligned} \tag{52}$$

Let us define $\Xi := \{w \mid \|w-\mathsf{w}^*\| \le 1\}$. We consider two cases.

Case 1: $w \in \Xi$. Since $0<\lambda_1<1$ and $\|w-\mathsf{w}^*\| \le 1$, consequently,

$$\|w-\mathsf{w}^*\|^2 - \|w-\mathsf{w}^*\|^{1+\lambda_1} \le 0.$$

Thus,

$$\dot{\mathcal{L}}(t,w(t)) \le -N_1\|w-\mathsf{w}^*\|^{1+\lambda_1} - N_2\|w-\mathsf{w}^*\|^{1+\lambda_2}, \tag{53}$$

where $N_1 = \frac{(\beta-\theta)\phi_1(t)}{(L+\theta)^{1-\lambda_1}} - q$, and $N_2 = (\beta-\theta)^{\lambda_2}\phi_2(t) - q$.

Case 2: $w \notin \Xi$. Since $\|w-\mathsf{w}^*\| > 1$ and $\lambda_2 > 1$, one has:

$$\|w-\mathsf{w}^*\|^2 - \|w-\mathsf{w}^*\|^{1+\lambda_2} \le 0,$$

and inequality (53) remains valid. Combining both cases gives:

$$\dot{\mathcal{L}}(t,w(t)) \le -\left(\frac{(\beta-\theta)}{(L+\theta)^{1-\lambda_1}}\phi_1(t)-q\right)\|w-\mathsf{w}^*\|^{1+\lambda_1} - \left((\beta-\theta)^{\lambda_2}\phi_2(t)-q\right)\|w-\mathsf{w}^*\|^{1+\lambda_2}.$$

Rewriting in terms of $\mathcal{L}$, we obtain:

$$\dot{\mathcal{L}}(t,w(t)) \le -2^{\frac{1+\lambda_1}{2}}\mathcal{F}_1(t)\mathcal{L}^{\frac{1+\lambda_1}{2}} - 2^{\frac{1+\lambda_2}{2}}\mathcal{F}_2(t)\mathcal{L}^{\frac{1+\lambda_2}{2}}.$$

where $\mathcal{F}_1 = \frac{(\beta-\theta)}{(L+\theta)^{1-\lambda_1}}\phi_1(t) - q$ and $\mathcal{F}_2 = (\beta-\theta)^{\lambda_2}\phi_2(t) - q$. Therefore, by Lemma 3, the trajectory $w(t)$ converges to w^* in FXT framework. □

Remark 4. *Assumption 2 imposes a state-dependent disturbance bound of the form*

$$\|D(w)\| < q\|w-\mathsf{w}^*\|,$$

where $w \neq \mathsf{w}^*$, which implies that the disturbance vanishes as the trajectory approaches the equilibrium point w^*. Therefore, the present robustness analysis guarantees FXT stability under vanishing bounded disturbances. The analysis does not directly cover genuinely bounded nonvanishing perturbations. Extending the proposed framework to accommodate persistent disturbances and practical FXT stability remains an interesting direction for future research.

6. Numerical Experiments

In this section, we investigate the performance of the proposed FXT-TVCNDM. By discretizing the continuous-time model (37) via the forward Euler method, we arrive at the following discrete scheme:

$$w_{k+1} = w_k - h_k \Gamma(w_k, t)\Big(\Upsilon(w_k) - \mathcal{P}_{\Phi(w)}(\Upsilon(w_k) - \eta w_k)\Big), \tag{54}$$

where $h_k > 0$ denotes the iteration-dependent step size, i.e., $h_k = h(k) > 0$ and initialize $w_0 \in \mathbb{R}^k$. The scaling factor $\Gamma(w_k, t)$ is defined as follows:

$$\Gamma(w_k, t) := \begin{cases} \dfrac{\phi_1(t)}{\|\Upsilon(w_k) - \mathcal{P}_{\Phi(w_k)}(\Upsilon(w_k) - \eta w_k)\|^{1-\lambda_1}} \\ \quad + \dfrac{\phi_2(t)}{\|\Upsilon(w_k) - \mathcal{P}_{\Phi(w_k)}(\Upsilon(w_k) - \eta w_k)\|^{1-\lambda_2}}, \text{ if } w_k \in \mathbb{R}^k \setminus \mathrm{Zer}(\Pi), \\ 0 \quad \text{otherwise,} \end{cases}$$

with $0 < \lambda_1 < 1$, $\lambda_2 > 1$, $\Pi(\cdot) = \mathcal{P}_{(\cdot)}(\Upsilon(\cdot) - \eta(\cdot)) - \Upsilon(\cdot)$, and $\phi_1(t), \phi_2(t) : [t_0, +\infty) \to \mathbb{R}_{++}$ are continuous functions for $k = 0, 1, 2, \ldots$. This discrete scheme provides an implementable iterative framework for solving the IQVIP.

6.1. One-Dimensional Numerical Example

We consider the following problem:

$$\Upsilon(w) = 3w + 1, \quad \Phi(w) = [g(w) - 1, g(w) + 1], \quad g(w) = \frac{1}{2 + |w|}.$$

The parameters are chosen as $\lambda_1 = 0.6$, $\lambda_2 = 1.4$, $\eta = 3$, $h = 0.005$. The introduction of time-varying coefficients $\phi_1(t)$ and $\phi_2(t)$ enhances the flexibility and adaptability of the proposed model as follows: $\phi_1(t) = 0.5 + \frac{0.8}{1+0.5t}$, $\phi_2(t) = 0.8\big(1 + 0.1\sin t\big)$. The algorithm is tested for multiple initial values in $[-3, 3]$.

The parameter values used in the one-dimensional numerical example and reported in Table 1 were carefully selected to maintain numerical stability and to demonstrate convergence behavior consistent with the theoretical FXT properties of the continuous-time model. As illustrated in Table 1 and Figures 1–3, all trajectories converge within a uniformly bounded number of iterations ranging approximately from 200 to 295 for different initial conditions, thereby validating the uniformly bounded convergence characteristics of the proposed framework. The iterative process was terminated when the stopping criterion $\|w^{k+1} - w^k\| < 10^{-5}$ was satisfied.

Table 1. Convergence iterations for different initial values.

Initial Value	Iterations k
−3.00	295
−2.57	289
−2.14	281
−1.71	271
−1.29	258
−0.86	238
−0.43	200
0.00	1

Table 1. *Cont.*

Initial Value	Iterations k
0.43	200
0.86	238
1.29	258
1.71	271
2.14	281
2.57	289
3.00	295

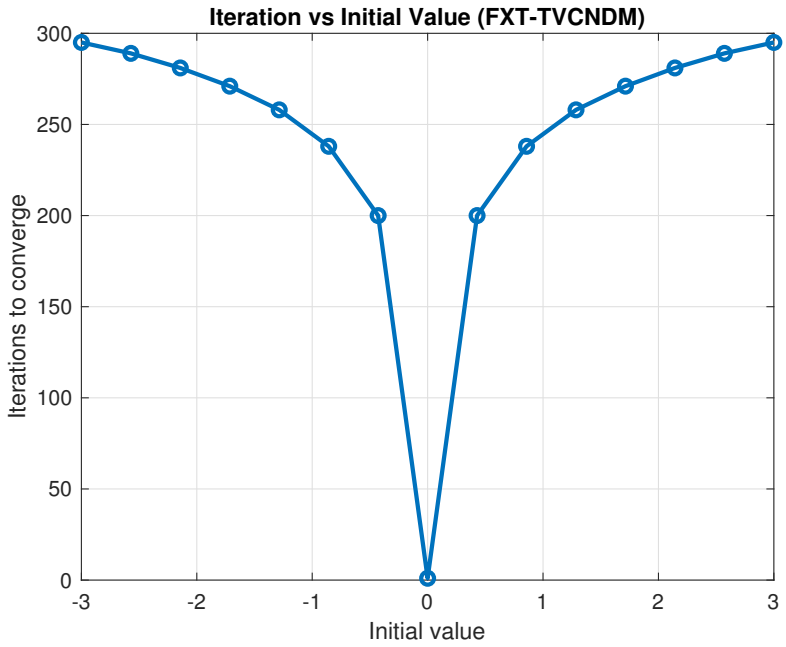

Figure 1. Iteration count versus initial value for the FXT-TVCNDM.

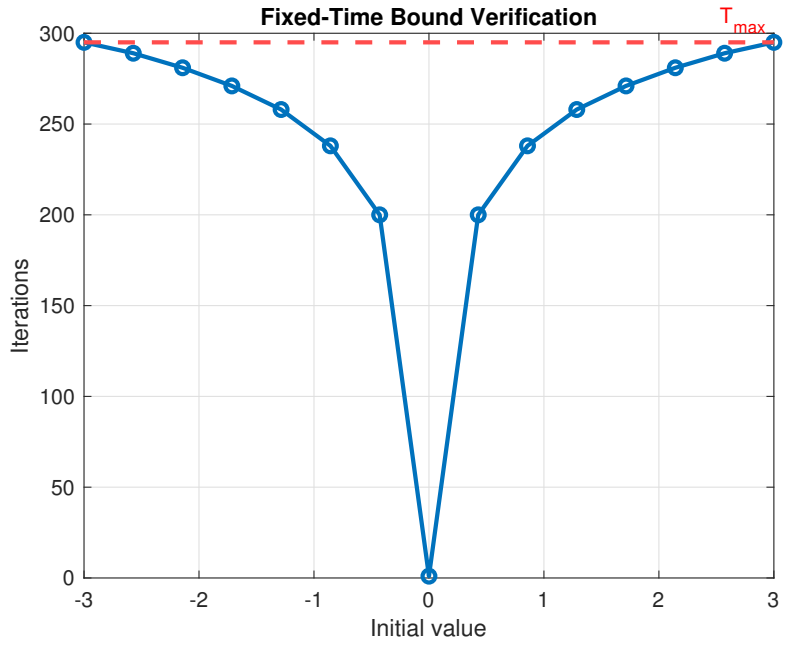

Figure 2. Verification of FXT property: all trajectories converge within the uniform bound $\mathcal{T}_{\max}$.

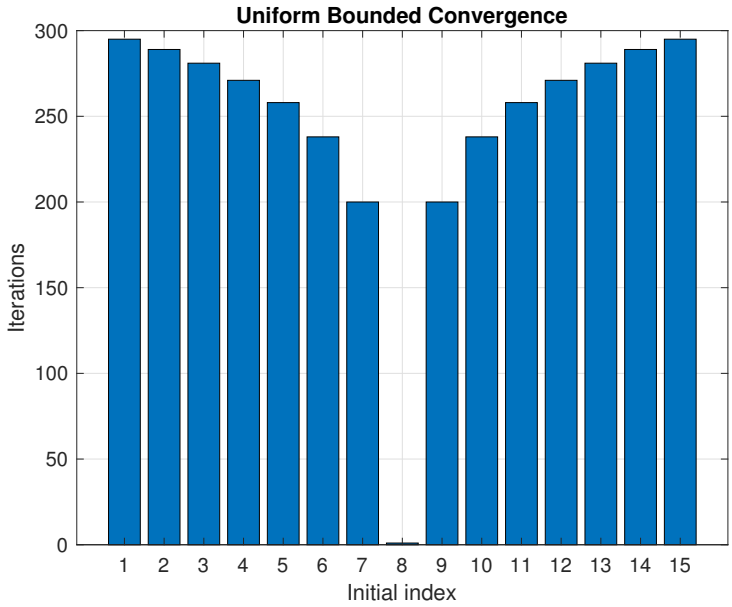

Figure 3. Bar plot of convergence iterations for different initial values.

From Table 1 and Figures 1–3, it is observed that all trajectories converge within a uniform upper bound $\mathcal{T}_{\max} = 295$. Although the convergence time varies with initial conditions, it remains uniformly bounded. This behavior is consistent with FXT convergence in the discrete setting. Therefore, the proposed FXT-TVCNDM demonstrates FXT convergence characteristics for solving IQVIPs. From Figure 4, it can be observed that the proposed time-varying coefficient framework (37) converges significantly faster than the constant-coefficient framework reported in [48] (see also Corollary 3, Case 1), thereby demonstrating improved convergence efficiency and transient performance. Specifically, for $\phi_1 = a_1 = 0.08$ and $\phi_2 = a_2 = 0.08$ with the same parameter of a one-dimensional example, the proposed approach reduces the number of iterations from 201 to 134, demonstrating improved convergence efficiency.

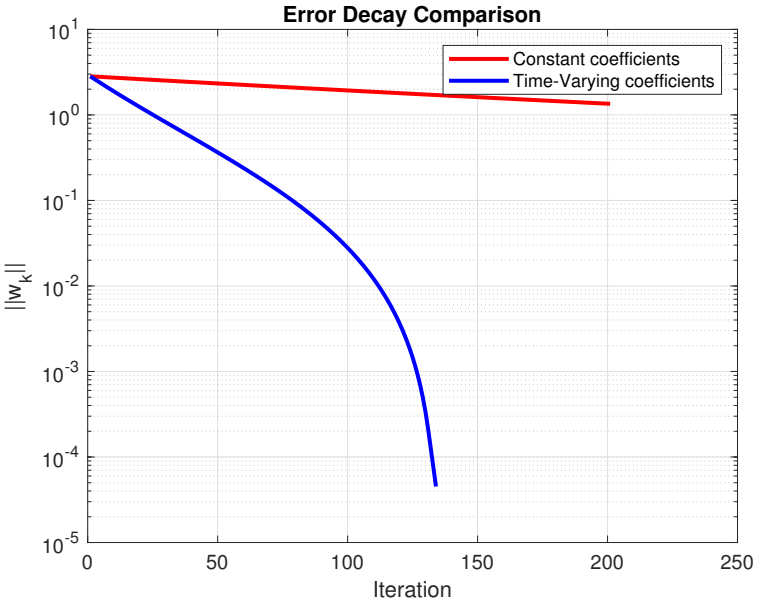

Figure 4. Comparison of convergence behavior for constant coefficient and time-varying coefficient models.

6.2. Two-Dimensional Numerical Example

To further demonstrate the scalability and applicability of the proposed framework, a two-dimensional IQVIP example was considered. The numerical implementation was carried out using the forward-Euler discretization scheme (54) associated with the proposed FXT-TVCNDM model. The parameters were chosen as $\lambda_1 = 0.6$, $\lambda_2 = 1.4$, $\eta = 3$, $h = 0.005$. The introduction of time-varying coefficients $\phi_1(t)$ and $\phi_2(t)$ enhances the flexibility and adaptability of the proposed model as $\phi_1(t) = \frac{1.2}{1+0.1t}$, $\phi_2(t) = (1 + 0.05 \sin t)$ with stopping tolerance $\|w^{k+1} - w^k\| < 10^{-4}$. The operator and state-dependent feasible set were defined by:

$$Q(w) = Aw + b, \quad \forall w = (w_1, w_2) \in \mathbb{R}^2,$$

where

$$A = \begin{pmatrix} 3 & -1 \\ -1 & 3 \end{pmatrix} \text{ is a symmetric matrix,} \qquad b = \begin{pmatrix} 1 \\ -1 \end{pmatrix}.$$

The state-dependent feasible set radius was chosen as $g(w) = \frac{0.5}{1+\|w\|}$. Accordingly, the feasible set was defined by:

$$\Phi(w) = \left\{ z = (z_1, z_2)^T \in \mathbb{R}^2 : |z_1| \leq g(w), |z_2| \leq g(w) \right\},$$

and the corresponding projection operator onto $\Phi(w)$ was implemented componentwise.

Different initial conditions were selected to investigate the convergence behavior of the iterative trajectories. The obtained numerical results corresponding to the two-dimensional IQVIP example are reported in Table 2. It can be observed that all trajectories converge successfully within a uniformly bounded number of iterations despite different initial values. In particular, the convergence iterations vary approximately from 86 to 259, which demonstrates stable and uniformly bounded convergence behavior consistent with the theoretical FXT properties of the continuous-time model. Moreover, the results further illustrate the robustness and scalability of the proposed time-varying coefficient framework in higher-dimensional settings.

Table 2. Iteration counts for the two-dimensional FXT-TVCNDM under different initial conditions.

Initial Condition w_0	Iterations Required
$(-3, -3)$	259
$(-2, -2)$	244
$(-1, -1)$	217
$(-0.5, 0.5)$	108
$(0, 0)$	86
$(0.5, -0.5)$	120
$(1, 1)$	217
$(2, 2)$	244
$(3, 3)$	259

The corresponding convergence behavior is illustrated in Figures 5–7. Figure 5 shows the variation in iteration counts for different initial conditions, while Figure 6 verifies the existence of a uniform upper bound on the convergence iterations. Figure 7 further illustrates the uniformly bounded convergence characteristics of the proposed FXT-TVCNDM framework.

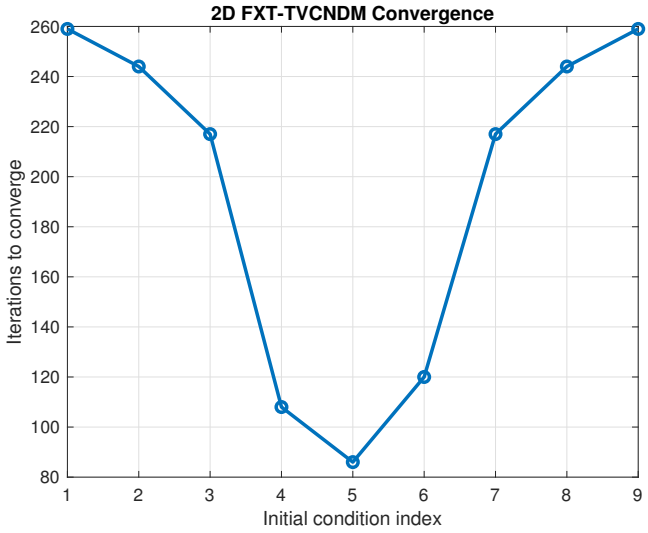

Figure 5. Iteration counts corresponding to different initial conditions for the two-dimensional FXT-TVCNDM.

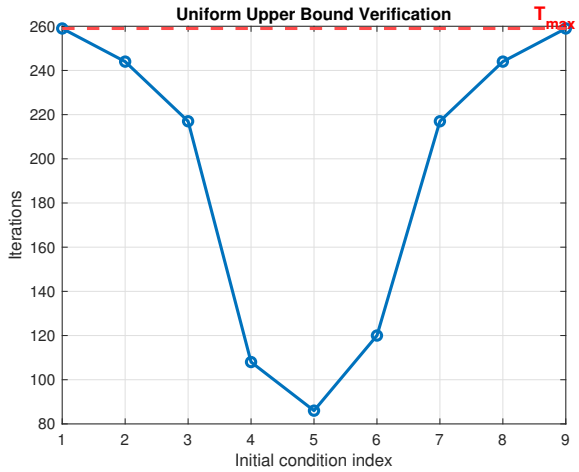

Figure 6. Verification of the uniform upper bound for the convergence iterations in the two-dimensional FXT-TVCNDM.

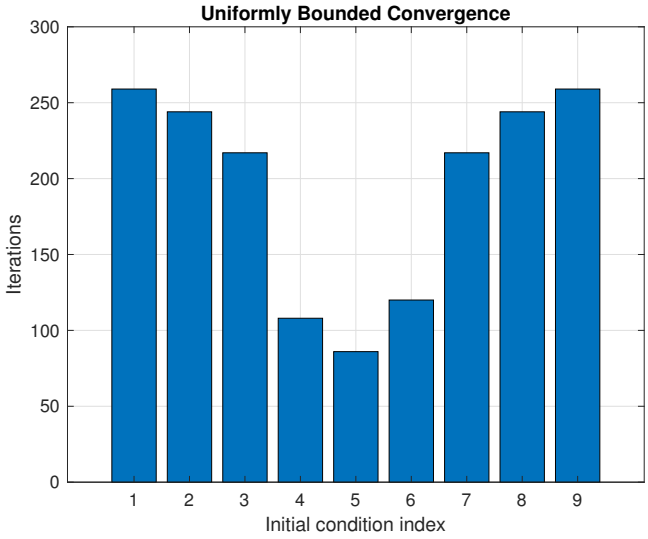

Figure 7. Uniformly bounded convergence behavior of the two-dimensional FXT-TVCNDM under different initial conditions.

7. Real-World Applications and Practical Implications of the Proposed Neurodynamic Framework

Although the proposed framework is formulated in a strict theoretical context, its construction is instinctively in line with an extensive body of real-world issues that can be framed as IQVIPs, as presented in (7). The combination of time-varying neurodynamic dynamics in (13) and their FT and FXT generalizations in (24) and (37) allows for a versatile and computationally feasible basis of practical implementation. Traffic equilibrium problems can be directly modeled in the IQVIP structure (7) in the transportation systems in which the feasible flow sets are determined by the prevailing state of a transportation system. The time-varying neurodynamic model (13) allows for adaptive convergence to the equilibrium, whereas the FXT formulation (37) allows convergence to be realized in a predictable time limit, which is especially beneficial in real-time traffic control and intelligent transportation systems. Resource allocation and congestion control in telecommunication networks can be formulated using IQVIP formulations, where network constraints are dynamically developed. The model (24) provides quick convergence and thus time-sensitive optimization problems including bandwidth allocation and load balancing can be effectively handled even in changing network conditions. From an engineering viewpoint, numerous optimization and control issues, e.g., energy management systems and distributed control architectures, can be viewed in terms of the operator-based structure of (13). The fact that the suggested models are strong when subjected to limited disturbances further increases their usefulness in the real world, where uncertainty and noise are inevitable. In multi-agent systems and robotics, coordination and decision-making issues tend to involve solving the equilibrium conditions under dynamical constraints. The issues may be traced into the IQVIP framework (7), which allows for offering the proposed neurodynamic models, especially the finite-time approach (24), where conversion is fast and reliable, which is essential in time-sensitive systems like motion planning and cooperative control. Moreover, adaptive optimization is central in the context of smart systems and Internet of Things (IoT) to ensure efficiency in the system. The time-varying gain structure in (13) enables the model to react well to the ongoing changing data streams, and stabilization over time (37) ensures the model is stable to constant performance irrespective of the initial state of the system. This renders the suggested structure especially applicable to the use of smart grids, intelligent monitoring systems, and real-time decision-support platforms. In general, the suggested neurodynamic model can close the divide between the theoretical developments in IQVIPs and the practical application of these concepts to various domains and provide a single and scalable solution to complex and real-time optimization challenges.

8. Results and Discussion

The numerical experiments confirm the effectiveness of the proposed FT-TVCNDM and FXT-TVCNDM frameworks. The results presented in Tables 1 and 2, together with Figures 1–3 and 5–7, show that all trajectories converge successfully within a uniformly bounded number of iterations under different initial conditions, thereby validating the FXT convergence behavior established theoretically. In particular, the obtained numerical results demonstrate stable and uniformly bounded convergence characteristics for both one-dimensional and two-dimensional IQVIP examples. Moreover, Figure 4 shows that the proposed time-varying coefficient framework achieves significantly faster error decay compared with the constant-coefficient scheme. This demonstrates the effectiveness of adaptive time-varying gains in improving convergence speed and transient performance. The additional two-dimensional numerical example further illustrates the scalability, robustness, and computational applicability of the proposed framework in higher-dimensional settings.

Overall, the numerical results confirm the robustness, stability, and computational efficiency of the proposed models, indicating their suitability for real-time optimization and engineering applications. It should also be noted that the observed convergence behavior of the discrete implementation is consistent with the FXT properties of the continuous-time model.

9. Conclusions

This paper developed FT and FXT neurodynamic models with time-varying coefficients for solving IQVIPs. The proposed framework establishes existence, uniqueness, global convergence, and explicit FT/FXT settling-time bounds using Lyapunov stability theory. In particular, the FXT models guarantee convergence within a uniform upper bound independent of initial conditions. A projection-based discretization scheme was also developed to obtain an implementable iterative algorithm. The numerical results presented in Tables 1 and 2, together with Figures 1–3 and 5–7, validate the theoretical FXT convergence characteristics of the proposed models under different initial conditions for both one-dimensional and two-dimensional IQVIP examples. Moreover, Figure 4 demonstrates that the proposed time-varying coefficient framework achieves faster convergence than the constant-coefficient scheme, highlighting the effectiveness of adaptive gains in improving convergence performance and transient behavior. Compared with the fractional SAQ alcohol stability model studied in [53], the proposed FXT-TVCNDM establishes explicit fixed-time convergence guarantees for IQVIPs together with adaptive time-varying dynamics and uniformly bounded convergence behavior. The proposed framework also demonstrates potential applicability in several real-world optimization and control problems, including traffic equilibrium, communication networks, distributed systems, and multi-agent coordination.

Future work will focus on extending the proposed models to large-scale and high-dimensional settings, as well as exploring data-driven and real-time implementations. Additionally, improved discretization strategies that better preserve fixed-time properties in numerical schemes remain an important direction for future research.

Author Contributions: Conceptualization: V.K.K. and M.K.A.; methodology: V.K.K.; supervision: M.K.A.; software: V.K.K.; investigation: V.K.K. and M.K.A.; validation: V.K.K. and A.A.; formal analysis: V.K.K. and A.A.; visualization: M.K.A. and A.A.; writing—original draft preparation: V.K.K.; writing—review and editing: V.K.K.; funding: A.A.; project administration: A.A. All authors have read and agreed to the published version of the manuscript.

Funding: This research received no external funding.

Data Availability Statement: No datasets were generated or analyzed during the current study.

Conflicts of Interest: The authors declare no conflicts of interest.

References

1. Facchinei, F.; Pang, J.S. *Finite-Dimensional Variational Inequalities and Complementarity Problems*; Springer-Verlag: New York, NY, USA, 2003; Volumes I and II.
2. Bauschke, H.H.; Combettes, P.L. *Convex Analysis and Monotone Operator Theory in Hilbert Spaces*; Springer: New York, NY, USA, 2011.
3. Censor, Y.; Gibali, A.; Reich, S. Extensions of Korpelevich's extragradient method for the variational inequality problem in Euclidean space. *Optimization* **2012**, *61*, 1119–1132. [CrossRef]
4. Malitsky, Y.V.; Semenov, V.V. An extragradient for monotone variational inequalities. *Cybern. Syst. Ananl.* **2014**, *50*, 271–277. [CrossRef]
5. Cao, Y.; Khan, V.K.; Sarfaraz, M.; Arbi, A.; Ahmad, M.K. Second-order dynamical system to solve the sum of monotone operators via the KM algorithm. *Alex. Eng. J.* **2025**, *123*, 341–345. [CrossRef]

6. Solodov, M.V.; Svaiter, B.F. A new projectional algorithm for variational inequality problems. *SIAM J. Control Optim.* **1999**, *37*, 765–776. [CrossRef]
7. Alam, M.A.; Irfan, S.S.; Ahmad, I. Convergence Properties and Numerical Illustration of a Resolvent-Based Inertial Extrapolation Method for Variational Inclusions in Banach Space. *Mathematics* **2025**, *13*, 3725. [CrossRef]
8. Collins, O.C.; Olanrewaju, O.A. Mathematical Model Analysis for Dynamics and Control of Yellow Fever and Malaria Disease Co-Infections. *Math. Comput. Appl.* **2026**, *31*, 21. [CrossRef]
9. Han, Y.; Huang, N.; Lu, J.; Xiao, Y. Existence and stability of solutions to inverse variational inequality problems. *Appl. Math. Mech.* **2017**, *38*, 749–764. [CrossRef]
10. Vuong, P.T.; He, X.; Thong, D.V. Global exponential stability of a neural network for inverse variational inequalities. *J. Optim. Theory Appl.* **2021**, *190*, 915–930. [CrossRef]
11. Zou, X.; Gong, D.; Wang, L.; Chen, Z. A novel method to solve inverse variational inequality problems based on neural networks. *Neurocomputing* **2016**, *173*, 1163–1168. [CrossRef]
12. He, B.; He, X.; Liu, H.X. Solving a class of constrained 'black-box' inverse variational inequalities. *Eur. J. Oper. Res.* **2010**, *204*, 391–401. [CrossRef]
13. He, X.; Liu, H.X. Inverse variational inequalities with projection-based solution methods. *Eur. J. Oper. Res.* **2011**, *208*, 12–18. [CrossRef]
14. Shi, L.; Xi, Q. Application of Generalized Finite Difference Method and Radial Basis Function Neural Networks in Solving Inverse Problems of Surface Anomalous Diffusion. *Math. Comput. Appl.* **2025**, *30*, 7. [CrossRef]
15. Aussel, D.; Gupta, R.; Mehra, A. Gap functions and error bounds for inverse quasi-variational inequality problems. *J. Math. Anal. Appl.* **2012**, *407*, 270–280. [CrossRef]
16. Dey, S.; Reich, S. A dynamical system for solving inverse quasi-variational inequalities. *Optimization* **2024**, *73*, 1681–1701. [CrossRef]
17. Gan, T.; Khan, V.K.; Ahmad, M.K.; Cai, Q.B. A second-order dynamical system for solving inverse quasi-variational inequalities and its application. *PLoS ONE* **2026**, *21*, e0344815. [CrossRef]
18. Chen, C.; Li, L.; Peng, H.; Yang, Y.; Mi, L.; Zhao, H. A new fixed-time stability theorem and its application to the fixed-time synchronization of neural networks. *Neural Netw.* **2020**, *123*, 412–419. [CrossRef]
19. Hu, X.; Wang, J. Global stability of a recurrent neural network for solving pseudomonotone variational inequalities. In Proceedings of the 2006 IEEE International Symposium on Circuits and Systems (ISCAS), Island of Kos, 21–24 May 2006; pp. 755–758.
20. Zheng, J.; Ju, X.; Zhang, N.; Xu, D. A novel predefined-time neurodynamic approach for mixed variational inequality problems and applications. *Neural Netw.* **2024**, *174*, 106247. [CrossRef]
21. Vuong, P.T. The global exponential stability of a dynamical system for solving variational inequalities. *Netw. Spat. Econ.* **2022**, *22*, 395–407. [CrossRef]
22. Bhat, S.P.; Bernstein, D.S. Finite-time stability of continuous autonomous systems. *SIAM J. Control Optim.* **2000**, *38*, 751–766. [CrossRef]
23. Ju, X.; Li, C.; He, X.; Feng, G. A proximal dynamic approach to equilibrium problems with finite-time convergence. *IEEE Trans. Autom. Control* **2023**, *69*, 1773–1780. [CrossRef]
24. Li, C.; Yu, X.; Huang, T.; Chen, G.; He, X. A generalized Hopfield network for nonsmooth constrained convex optimization: Lie derivative approach. *IEEE Trans. Neural Netw. Learn. Syst.* **2015**, *27*, 308–321. [CrossRef]
25. Polyakov, A. Nonlinear feedback design for fixed-time stabilization of linear control systems. *IEEE Trans. Autom. Control* **2012**, *57*, 2106–2110. [CrossRef]
26. Garg, K.; Baranwal, M.; Gupta, R.; Benosman, M. Fixed-time stable proximal dynamical system for solving MVIPs. *IEEE Trans. Autom. Control* **2022**, *68*, 5029–5036. [CrossRef]
27. Ju, X.; Hu, D.; Li, C.; He, X.; Feng, G. A novel fixed-time converging neurodynamic approach to mixed variational inequalities and applications. *IEEE Trans. Cybern.* **2021**, *52*, 12942–12953. [CrossRef] [PubMed]
28. Sánchez-Torres, J.D.; Loza-Lopez, M.J.; Ruiz-Cruz, R.; Sanchez, E.N.; Loukianov, A.G. A fixed time convergent dynamical system to solve linear programming. In *53rd IEEE Conference on Decision and Control*; IEEE: Piscataway, NJ, USA, 2014; pp. 5837–5842.
29. Wang, H.; Xu, K.; Qiu, J. Event-triggered adaptive fuzzy fixed-time tracking control for a class of nonstrict-feedback nonlinear systems. *IEEE Trans. Circuits Syst. Regul. Pap.* **2021**, *68*, 3058–3068. [CrossRef]
30. Wang, H.; Liu, P.X.; Zhao, X.; Liu, X. Adaptive fuzzy finite-time control of nonlinear systems with actuator faults. *IEEE Trans. Cybern.* **2019**, *50*, 1786–1797. [CrossRef] [PubMed]
31. Wang, H.; Bai, W.; Zhao, X.; Liu, P.X. Finite-time-prescribed performance-based adaptive fuzzy control for strict-feedback nonlinear systems with dynamic uncertainty and actuator faults. *IEEE Trans. Cybern.* **2021**, *52*, 6959–6971. [CrossRef] [PubMed]
32. Zuo, Z.; Han, Q.L.; Ning, B.; Ge, X.; Zhang, X.M. An overview of recent advances in fixed-time cooperative control of multiagent systems. *IEEE Trans. Ind. Inform.* **2018**, *14*, 2322–2334. [CrossRef]
33. Benosman, M.; Romero, O.; Cherian, A. Optimizing deep neural networks via discretization of finite-time convergent flows. *arXiv* **2020**, arXiv:2010.02990.

34. Cortés, J. Finite-time convergent gradient flows with applications to network consensus. *Automatica* **2006**, *42*, 1993–2000. [CrossRef]
35. Garg, K.; Panagou, D. Fixed-time stable gradient flows: Applications to continuous-time optimization. *IEEE Trans. Autom. Control* **2021**, *66*, 2002–2015. [CrossRef]
36. Nguyen, L.T.; Eberhard, A.; Yu, X.; Kruger, A.Y.; Li, C. Finite-time nonconvex optimization using time-varying dynamical systems. *J. Optim. Theory Appl.* **2024**, *203*, 844–879. [CrossRef]
37. He, X.; Wen, H.; Huang, T. A fixed-time projection neural network for solving the L_1 minimization problem. *IEEE Trans. Neural Netw. Learn. Syst.* **2022**, *33*, 7818–7828. [CrossRef]
38. Xu, J.; Li, C.; He, X.; Zhang, X. Projection neural networks with finite-time and fixed-time convergence for sparse signal reconstruction. *Neural Comput. Appl.* **2024**, *36*, 425–443. [CrossRef]
39. Garg, K.; Baranwal, M. Continuous-time accelerated proximal point algorithm for sparse recovery. *IEEE Signal Process. Lett.* **2020**, *27*, 1760–1764. [CrossRef]
40. Yu, L.; Zheng, G.; Barbot, J.P. Dynamic sparse recovery with finite-time convergence. *IEEE Trans. Signal Process.* **2017**, *65*, 6146–6157. [CrossRef]
41. Ju, X.; Che, H.; Li, C.; He, X.; Feng, G. Exponential convergence of a proximal projection neural network for mixed variational inequalities and applications. *Neurocomputing* **2021**, *454*, 54–64. [CrossRef]
42. Ju, X.; Li, C.; Che, H.; He, X.; Feng, G. A proximal neurodynamic network with fixed-time convergence for equilibrium problems and its applications. *IEEE Trans. Neural Netw. Learn. Syst.* **2022**, *34*, 7500–7514. [CrossRef]
43. Dar, A.H.; Younis, M.; Chen, L. Convergence Analysis for Approximating Solution of Variational Inclusion Problem. *Facta Univ. Ser. Math. Inform.* **2023**, *38*, 659–669. [CrossRef]
44. Younis, M.; Dar, A.H.; Hussain, N. Revised algorithm for finding a common solution of variational inclusion and fixed point problems. *Filomat* **2023**, *37*, 6949–6960. [CrossRef]
45. Nguyen, L.T.; Yu, X.; Eberhard, A.; Li, C. Fixed-time gradient dynamics with time-varying coefficients for continuous-time optimization. *IEEE Trans. Autom. Control* **2022**, *68*, 4383–4390. [CrossRef]
46. Ju, X.; Yang, X.; Yuan, S.; Ho, D.W. Fixed-time neurodynamic optimization approach with time-varying coefficients to variational inequality problems and applications. *Commun. Nonlinear Sci. Numer. Simul.* **2025**, *140*, 108414. [CrossRef]
47. Feng, L.; Ju, X.; Lu, J.; Yang, X. Inverse-free neurodynamic optimization approach with time-varying coefficients for absolute value equations and its FPGA circuit implementation. *Commun. Nonlinear Sci. Numer. Simul.* **2026**, 156, 109672. [CrossRef]
48. Van Tran, N.; Le, T.T.H. Finite-time and fixed-time stable dynamical systems for solving inverse quasi-variational inequality problems. *Optimization* **2026**, 1–23. [CrossRef]
49. Karamardian, S.; Schaible, S. Seven kinds of monotone maps. *J. Optim. Theory Appl.* **1990**, *66*, 37–46. [CrossRef]
50. Kinderlehrer, D.; Stampacchia, G. *An Introduction to Variational Inequalities and Their Applications*; Society for Industrial and Applied Mathematics: Philadelphia, PA, USA, 2000.
51. Pappalardo, M.; Passacantando, M. Stability for equilibrium problems: From variational inequalities to dynamical systems. *J. Optim. Theory Appl.* **2002**, *113*, 567–582. [CrossRef]
52. Alwan, M.S.; Liu, X. *Theory of Hybrid Systems: Deterministic and Stochastic*; Higher Education Press: Beijing, China, 2018.
53. Öztürk, Z.; Bilgil, H.; Sorgun, S. Fractional SAQ alcohol model: Stability analysis and Türkiye application. *Int. J. Math. Comput. Eng.* **2025**, *3*, 125–136. [CrossRef]

Disclaimer/Publisher's Note: The statements, opinions and data contained in all publications are solely those of the individual author(s) and contributor(s) and not of MDPI and/or the editor(s). MDPI and/or the editor(s) disclaim responsibility for any injury to people or property resulting from any ideas, methods, instructions or products referred to in the content.